Proceedings of the SURVEYING & SPATIAL SCIENCES BIENNIAL CONFERENCE 2011
21-25 November 2011, Wellington, New Zealand

Automated Matching of Segmented Point Clouds to As-built Plans

David Belton[1,2], Brian Mooney[2], Tony Snow[2] and Kwang-Ho Bae[3]
[1]CRC for Spatial Sciences
[2]Department of Spatial Sciences, Curtin University
GPO BOX U1987, Perth, Western Australia, 6845, Australia
[3]Fugro Spatial Solutions Pty Ltd,
18 Prowse Street, West Perth, WA, 6005, Australia
d.belton@curtin.edu.au, brian.mooney@student.curtin.edu.au, t.snow@curtin.edu.au,
k.h.bae@furgospatial.edu.au

ABSTRACT

Terrestrial laser scanning (TLS) is seeing an increase use for surveying and engineering applications. As such, there is much on-going research into automating the process for segmentation and feature extraction. This paper presents a simple method for segmenting the interior of a building and comparing it to as-built plans. The method is based on analysing the local point attributes such as curvature, surface normal direction and underlying geometric structure. Random sampling consensus (RANSAC), region growing and voting techniques are applied to identify the predominant salient surface feature to extract wall and vertical segments. This information is used to generate a 2D plan of the interior space. A distance weighted method then automatically locates the corresponding vertices between the different datasets to transform them into a common coordinate system. A traditional survey was performed alongside the 3D point cloud capture to compare and validate the generated 2D plans and the comparison to the existing drawings. The accuracy of such generated plans from 3D point clouds will be explored.

KEYWORDS: Terrestrial Laser Scanning, Segmentation, 3D Point Cloud, Matching

1 INTRODUCTION

Laser Scanners enable users to sample dense three-dimensional (3D) point data from surfaces with high spatial resolution, which allow for the representation and modelling of salient features. This raw point data is commonly referred to as point clouds, and with post-processing can be converted into model or vector format and salient information can be resolved. Terrestrial Laser Scanning (TLS) has gained popularity in areas such as 3D-reconstruction of terrain (Frank et al., 2007), deformation monitoring (Gordon, 2005), building segmentation (Miliaresis et al., 2007) industrial modelling (Rabbani and van den Heuvel, 2004), and other conventional surveying applications.

The need for reconstruction of building environments has lead to the research in developing automation techniques. Examples of such techniques are based on recognising geometric structure (Vosselman and Dijkman, 2001), sweeping vertical plans to detect wall features (Budroni A. and Böhm, 2009), random sampling and Hough transforms for detecting elements (Tarsha-Kurdi et. al., 2007), 2D density histogram for detecting the occurrence vertical features (Okorn et. al., 2010) and region growing on the surface normal direction (Rabbani et. al., 2006).

This has lead to investigations on the comparative ability of TLS with traditional techniques and practices. The systematic errors for TLS are, in principle, the same as that of an EDM instrument, which is extensively described by Rüeger (1990). Even with their increased usages in the surveying industry, there are still questions concerning the spatial quality of the information

captured by Terrestrial Laser Scanners, especially in terms of accuracy. Studies on the positional accuracy of terrestrial laser scanners have been conducted in the past (Boehler et al. 2003, G. Mólnar et al. 2009, Lichti 2007). There has been few studies on the comparison between traditional surveying and laser scanners (e.g. Lichti et al. 2005, Froehlich and Metternleiter 2004), especially in the area of studies with respect to as-constructed surveys.

This paper aims to automatically extract 2D drawings, and analyse conventional total station surveys and Terrestrial Laser Scanning surveys compared to as-constructed plans. This is done in order to demonstrate that the Terrestrial Laser Scanner can be used as a comparable surveying method for indoor applications.

2 METHODOLOGY

The test site used for the procedures outlined in this paper was located on the third level of the Department of Spatial Sciences at Curtin University. Workflow consisted of three stages; acquisition of the data and control network by survey and TLS, processing the 3D data to produce a 2D drawing, and aligning and comparing the 2D drawing with the control survey and as-built plans in terms of accuracy. The control survey allows for generating as-built plans using traditional techniques for comparison, alignment of the point cloud to the plans, and geo-referencing the different aspects to a global coordinate system, which in this case was MGA94 and AHD94 for the easting and northing components, and the elevation component, respectively. Processing of the TLS point cloud data is aimed at automatically producing a 2D line drawing representation of the data, and defining vertices and control points that are common between the control and as-built survey, and the 2D plans. An automated method of comparing the network of control points and vertices is used by examining the distance matrix between the different elements, and finding the most likely corresponding elements between the datasets.

2.1 Control survey

While not a necessary component of the project, to allow for geo-referencing of the point cloud data, a control network was established by traversing between two local survey marks and using the two shaft method (Anderson and Mikhail, 1998). This method involves having two wires separated by the longest distance possible, in this case 110m, with known coordinates established from adjacent surface control. A traverse was then carried out between the two wires using control points placed in strategic locations of the third floor of the building. This method was chosen over other shaft plumbing methods, e.g. the Weisbach triangle method, because it produces a lower orientation error (Anderson and Mikhail, 1998; Schofield and Breach, 2007).

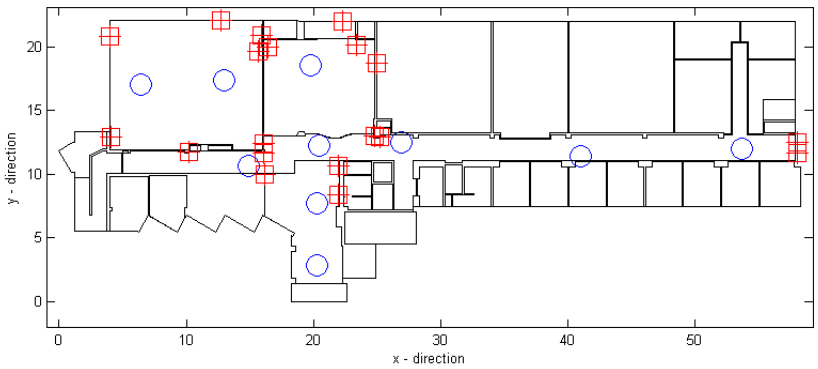

Figure 1: 2D plan with scanner setups represented by blue circles and geo-referenced targets denoted by red crosses.

This method allows the placement of a network of 19 targets for registering the separate scans into a local coordinate system, and to align the registered point cloud to a global coordinate system. Figure 1 shows the placement of these targets relative to the building scans. These 19 geo-referenced targets (black and white Leica paper targets) were placed and positioned utilising a Sokkia total station (Set530RK3; Sokkia, 2011). The measurements were carried out in reflector-

less mode, and measured 5 times with the results averaged to and adjusted. Targets were acquired within an accuracy of ±(3mm + 2ppm) for the distance and 5" for the angle. To align and compare the point cloud, control survey and the 2D plans together in a common coordinate system, a control survey was also conducted to generate vertices representing the corners and intersection of walls.

2.2 Point cloud acquisition

The point cloud of the test site was captured using a Leica Scanstation (Leica 2011). Due to the need to traverse through narrow corridors, 10 setups were used to ensure adequate coverage and capture of the interior. The locations of these stations are represented in Figure 1 by the blue circles. The network of 19 geo-referenced targets outlined in the previously section were used to register the separate scans setup into a single point cloud which is tied into the absolute coordinate. 3D point cloud post-processing software provides a set of semi-automatic tools for this registration procedure. In this case, Cyclone (Leica, 2011) was utilised which can detect both reflective and paper-based targets. Once all the targets are detected and labelled, the Cyclone software utilises an iterative processing method to find the optimal transformation solutions for each set of point clouds, e.g. the ICP and its variants (Bae and Lichti, 2008).

Table 1: Statistics on the differences between control points by total station (geo-referenced) and registered point cloud.

	ΔEasting (m)	**ΔNorthing (m)**	**ΔHeight (m)**
Mean	-0.2564×10^{-4}	-0.5128×10^{-4}	-0.2564×10^{-4}
Standard Deviation	0.001724	0.001605	0.001953

Although the Cyclone software can successfully detect targets in an automated manner, there can be instances where features present in the point cloud are incorrectly identified as targets. As such, a manual inspection or outlier detection method is used to identify and remove such occurrences. The final registration error is presented in Table 1, which shows the mean registration error is in the order of 2mm. This is well within the expected positional error for the Leica Scanstation. The registered point clouds for this experiment are presented in Figure 2.

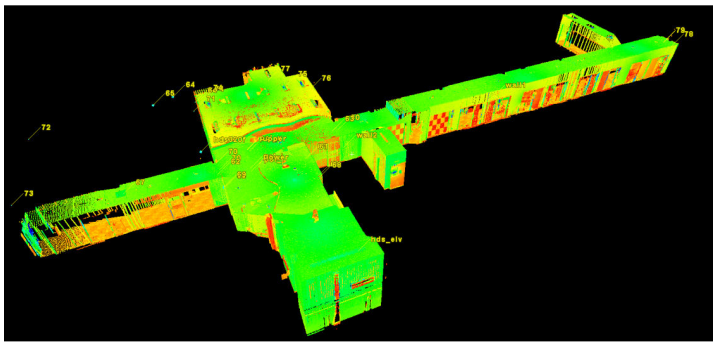

Figure 2: Registered point cloud of corridors on level three of the spatial sciences building.

In order to compare the geo-registered 3D point clouds and the CAD model, a 2D line model must be derived from 3D point cloud data. This transformation calculated between the x and y coordinates of the 2D drawings and the Easting and Northing components of the 3D point. Automated methods for performing this are outlined in the following sections.

3 AUTOMATED SEGMENTATON AND FEATURE IDENTIFICATION

The manual extraction of features is a labour intensive task. Therefore, much research has focused in the development of automated methods of segmenting and extracting features from

point clouds. When the objective is to derive the 2D plan, the process becomes much simpler as extraction methods are focused mainly on identifying and isolating vertical surfaces that correspond to walls, windows, doorways and other vertical features relevant to 2D drawings. The method outlined in this section is divided into two stages. The first stage is to identify all points that are potentially sampled from a vertical surface, and segment them into continuous regions. The second stage is to model these regions into 2D elements, and identify features that will comprise of vertices in a 2D drawing. These will allow for a comparison to be made with the as-built plans and the control survey by matching corresponding features between the different data sources.

3.1 Data processing and Region growing

Since the aim is to identify points that are candidates associated with walls, a method to classify such points is based on the local surface normal and surface curvature. A simple method used to derive this information is by fitting a planar surface to the local neighbourhood surrounding each point using principal component analysis (PCA) (Johnson and Wichern, 2002), and using the surface variance to determine the local curvature. Applying PCA produces a covariance matrix for a local neighbourhood such that:

$$C = \frac{1}{k-1}\sum_{i=1}^{k}(p_i - \bar{p})(p_i - \bar{p})^T \quad (1)$$

where p_i is defined as the vector form of the position of the i^{th} point in the neighbourhood containing the nearest k points and $\bar{p}$ represents the centroid of the neighbourhood calculated as the mean of the neighbourhood. The covariance matrix can be represented by eigenvalue decomposition such that the real positive eigenvalues, λ_0, λ_1 and λ_2, along with the corresponding eigenvectors e_0, e_1 and e_2 form an orthogonal basis of the neighbourhood in R^3 (Golub and Loan, 1989). The covariance matrix C can be decomposed as follows:

$$C = \sum_{i=0}^{2}\lambda_i e_i e_i^T \quad (2)$$

where $\lambda_0 \leq \lambda_1 \leq \lambda_2$. Note that eigenvectors e_i represent the principal components, with the corresponding eigenvalues λ_i denoting the variance in these directions (Golub and Loan, 1989). For a local neighbourhood of a point cloud, e_0 approximates the local surface (Pauly et al., 2002). This result is equivalent to the first order least squares plane fit (Shakarji, 1998). From this, an approximation for the surface curvature can be specified, as presented in Pauly et al. (2002), by the following:

$$\kappa \approx \sigma_n^2(p) = \frac{\lambda_0}{\lambda_0+\lambda_1+\lambda_2} \quad (3)$$

Using this information, a point can be classified as a likely candidate to have been sampled from a wall if the surface normal is approximately orthogonal to the vertical direction and the surface is locally flat (i.e. the surface curvature is nominally zero). Thresholds can be applied to test for this attributes. Figure 3(a) shows such classified point with the following thresholds:

$$\begin{aligned} \kappa_i &\approx \sigma_n^2(p) && < 0.001 \\ \theta_i &= |90 - \arccos(n_i[z])| && < 5^o \end{aligned} \quad (4)$$

where $n_i[z]$ is the vertical component of the normal direction for point p_i. To refine this information, a technique such as the random sampling consensus method (RANSAC) can be applied (Fischler and Bolles, 1981). This method iteratively selects random sub-samples from the local neighbourhood and fits a surface (in this case a plane) to find a set of points that are within a set tolerance of the points (termed the consensus set). The plane with the largest number of points in the consensus set is selected as the best fit, and the associated points will have the surface attributes of the fitted plane. If points do not belong to any consensus set, it can be said that they are not sampled from a locally planar surface.

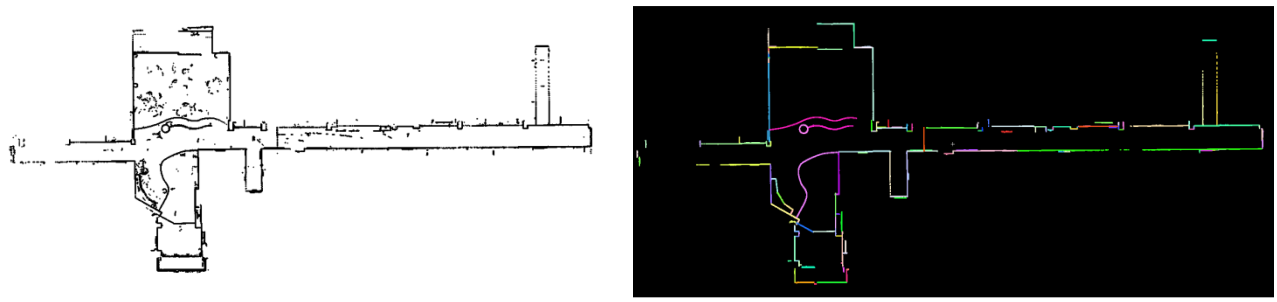

(a) (b)

Figure 3: (a) the classified points that are likely sampled from vertical surfaces. (b) the segmented points of different vertical surfaces. Different colours denotes different surface segments.

From these classified points, continuous surface segments can be extracted to determine the sampled points that belong to each vertical wall feature. There are several options to segment classified points. Some of these include clustering or analysing in the normal orientations (Budroni and Böhm, 2009), Hough transformations (Vosselman and Dijkman, 2001), RANSAC for shape and region extraction (Schnabel et. al., 2007). In this paper, a simple region growing method was applied on the normal and curvature values to segment the points into regions representing smooth surfaces (Rabbani et. al., 2006).

The region growing process starts by selecting a seed point from the previously classified points. Points in the local neighbourhood (within a certain range) around the point of interest are examined based on the difference between normal directions and the distance between them in the normal direction. Those points in the neighbourhood where both attributes are within a set tolerance to those of the point of interest (nominally zero) are added to the same segment as the point of interests. A new point of interest is selected from the added points until all such points have been examined, and no additional points can be used. A new seed point is selected and the procedure repeated until every point has been visited. Segments with an insignificant amount of points are ignored. Figure 3(b) shows the results of the procedure applied to the test data set. Refinements to the segmentation process can be made by including curvature, principle directions and boundary conditions (Belton and Lichti, 2006).

3.2 2D plan extraction and Feature identification

Because the point cloud has been orientated to the horizontal plane, the vertically aligned features will be of importance to generating the 2D plans (for example, walls doorways, windows, pillars, etc). As such, the previously classified points and segments can now be examined in the 2D horizontal domain (the x-y axis or easting and northing). If the raw points are examined, then the walls can be extracted by using voting techniques on the normal direction and point location (Knuth, 1999). This can be done by examining the angular direction (α_i) and distance (δ_i) from the origin for every point, which is defined by:

$$\delta_i = \sqrt{(x_i - x_0)^2 + (y_i - y_0)^2} \qquad (5)$$
$$\alpha_i = \arctan\left(\frac{n_i[x]}{n_i[y]}\right)$$

where x_i and y_i are from the coordinates of the i^{th} point, x_0 and y_0 are from the coordinates of the origin, and $n_i[x]$ and $n_i[y]$ are the corresponding x and y elements of the normal direction respectively. A clustering algorithm can then be applied to find concentration of points with similar parameters, similar to the Gaussian sphere approach in 3D (Várady, 1998). These clusters of points can then be modelled as a continuous line segment. Similarly Hough transformations (Vosselman and Dijkman, 2001) can be applied to the 2D point coordinates, similar to those mentioned in the previous sections (Budroni and Böhm, 2009), as well as a region growing process on the attributes described in Equation 5. Since the points have already been segmented, these procedures are not necessary in this instance. However, they are mentioned because if the sample density of the points is too sparse in the 3D domain, using the described methods in this section

may produce more robust results as the sample density in just the 2D horizontal domain will be higher than in the 3D domain.

For each of the segments, a line is fitted to the 2D points using PCA on the x and y coordinates, to get a mean point to represent the centre (c_j) of the line and with the associated direction (d_j). If the RMS value for the line fit is significantly large, then the segment can be categorised as a non-straight line segment. In this case, other line types can be fitted such as circles, arcs or splines, using least squares. For a point *i* belonging to a straight line segment *j*, the distance along the line segment can be specified as:

$$s_i = \big(x_i - c_j[x]\big)d_j[x] + \big(y - c_j[y]\big)d_j[y] \quad (6)$$

The points with the largest and smallest values of s_i denote the extents (p_1 and p_2) of the straight line segment such that:

$$p_1 = c_j + s_{min}d_j$$
$$p_2 = c_j + s_{max}d_j \quad (8)$$

These points can then be used to create the line segment for the 2D plan drawing, as shown in Figure 4 (a). To extend these line segments, the extents of a line segment are tested to determine if it is close to another line segment. If it is, then it is likely that the extent can be modified to extend and intersect to the other nearby line segment. These cases are illustrated in Figure 5 (a) and (b). If the directions of the lines are nominally aligned, the two segments likely belong to the same element and are merged together to create a new segment, as shown in Figure 5 (c). For the case where the line extents are close to one another (within a specified tolerance), but the directions differ significantly, then the intersection of the two lines can be calculated. This intersection can then define the new extents of both lines. Figure 4(b) shows the results of applying this procedure to the initial line segments from Figure 4(a).

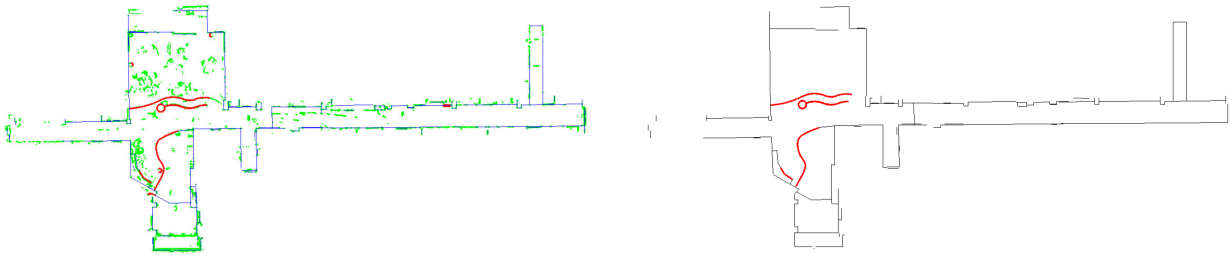

(a) (b)

Figure 4: (a) the initially extracted 2D straight lines (blue), extracted splines for non-straight segments (red), and the raw points (green). (b) the final extracted 2D drawings, with straight lines (black), and more complicated sections modeled by splines (red)

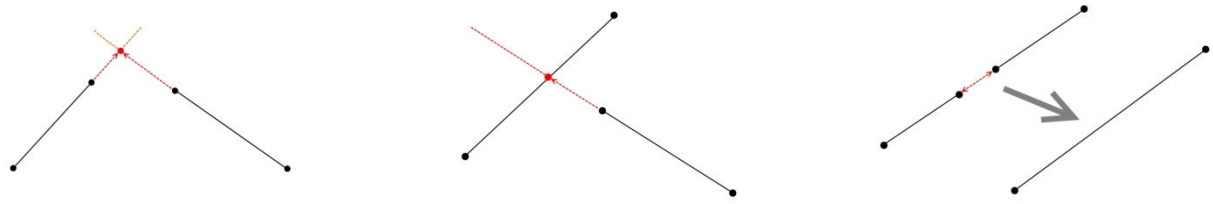

(a) (b) (c)

Figure 5: (a) Extending antwo lines to intersection, (b) extending the extent of a line to another line segment, and (c) merging two nominally align sections

These intersections can be matched to corresponding vertices in the as-built plans and used to align the three representations (point cloud, survey and as-built drawings) together for comparison. As can be seen in Figure 4, there are missing elements from the 2D drawings, and not all the information is captured. One reason for this is that the corridor consisted of large glass

sections which could not be captured. Another reason is that, due to the narrow corridors, the average point density was quite sparse in some areas. Additional setups and a finer scanning resolution will help achieve a greater level of detail.

4 AUTOMATED CORRESPONDENCE

In this section, a method for aligning the different datasets is presented utilising a method based on the voting algorithm (Knuth, 1999). The procedure is similar to those employed in calibration and registration techniques for aligning separate overlapping point clouds. The method comprises of several steps, the first is to isolate points that will be used for correspondence between the data sets. In this case, such points will comprise of the surveyed targets and the corner vertices representing the intersection between walls. An initial correspondence between the points is then found by examining the relationship between points in a data set, based on the distances between them. Once the vertices have been match, the different data sets can be transformed into a common coordinate system for comparison.

4.1 Correspondence matrix and Vertex Matching

Different properties, such as geometric invariant properties (Sharp et al., 2002), (e.g. curvature, moment and spherical harmonics invariants), can be used to find correspondence between the data. The only requirement is that the attributes are observable between different data sets. Similarly, the vertices can be chosen using different geometric or spectral properties to extract feature points, such as using mean and Gaussian curvature to define points of local minimums and maximums (Beinat et. al., 2007). In this case, the vertices used are the surveyed targets and the extracted and identified vertices representing corners of walls. The distances between the points within a dataset are used to find correspondence by searching for similar distances occurring in multiple data sets.

The first step, given the dataset $S^{(1)}$, is to calculate a distance matrix $D^{(1)}$ where the i^{th} row and the j^{th} column in the matrix contains the Euclidean distance between the vertices p_i and p_j such that:

$$D^{(k)}{}_{i,j} = \|p_i - p_j\|, \quad given\ (p_i, p_j)\ \epsilon\ S^{(k)} \tag{9}$$

The distance values in $D^{(1)}$ and $D^{(2)}$ are compared to determine if the values between two observed points in $D^{(1)}$ and two observed in the $D^{(2)}$ are within a specified tolerance. A voting method is used where vertices between datasets, if the same distance to another vertex is being observed, then the likely correspondence is increased by one. The follow algorithm explains the procedure for producing the correspondence matrix C:

Procedure for Correspondence Matrix

1. Read in set $S^{(1)}$ comprising of n points;
2. Read in set $S^{(2)}$ comprising of m points;
3. Create $D^{(1)}$ and $D^{(2)}$;
4. Create zero n by m matrix C;
5. For i1 = 1 to n
6. For j1 = 1 to n
7. For i2 = 1 to m
8. For j2 = 1 to m
9. If $(D^{(1)}_{i1,j1} - D^{(2)}_{i2,j2}) < \text{tol}$
10. $C_{i1,j1} = C_{i1,j1} + 1$;
11. End
12. End
13. End
14. End
15. End

Algorithm 1: The voting method for determining the correspondence matrix

This produces a correspondence matrix between the plans and the point cloud for the test site as specified in Figure 6. If there is a high value between the i^{th} row and the j^{th} column in C, then this indicates the likelihood of a high correspondence between the point p_i in set $S^{(1)}$, and the point p_j in set $S^{(2)}$. For each p_i in set $S^{(1)}$, the p_j in set $S^{(2)}$ is initially selected as the matching vertex if it has the highest correspondence value in row i^{th}, and the value is significantly large. If a point p_j in set $S^{(2)}$ is associated with more than one point in set $S^{(1)}$, then the point pair with the highest correspondence entry is kept, and the others removed. These matching pairs are then used to determine the transformation parameters used to align the datasets together. The matching pairs are presented in Figure 7. While this example is for 2D data, the process can be easily used for 3D data as well, since the correspondence is a simple distance metric.

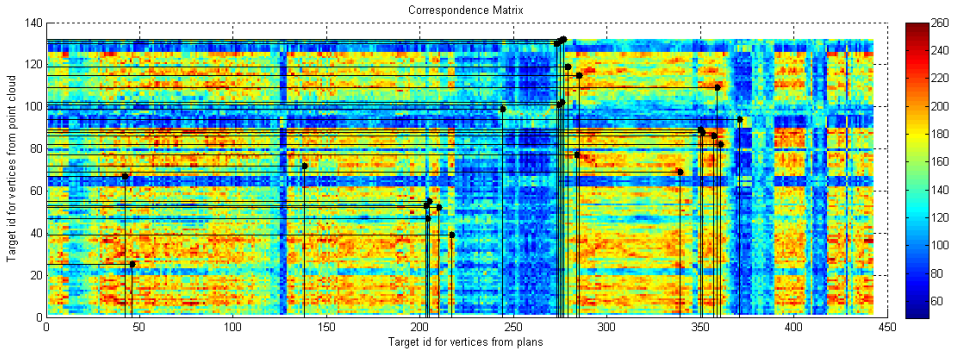

Figure 6: The correspondence matrix for the test site. Red values indicate a high correspondence between the vertices in the point cloud (vertical axes) and the vertices from the as-built plans (horizontal axis).

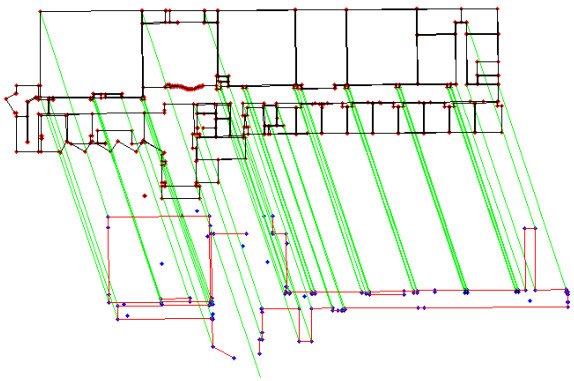

Figure 7: The initially matched vertices selected from the correspondence matrix.

4.2 Alignment and Refining Matching

To find the alignment, the problem is defined as a 2D rigid body transformation. In this case, the parameters will represent a rotation (θ) and two translations (x_t and y_t) such that:

$$\begin{bmatrix} x_i \\ y_i \end{bmatrix} = \begin{bmatrix} cos\theta & sin\theta \\ -sin\theta & cos\theta \end{bmatrix} \begin{bmatrix} u_i \\ w_i \end{bmatrix} + \begin{bmatrix} x_t \\ y_t \end{bmatrix} \quad (10)$$

The parameters are solved using least squares to determine the alignment between different data sets. After an initial solution is found, errors in the match vertices are detected as outliers if they are outside a specified confidence interval. Such errors are removed from the set of matched vertices. Similarly, there may be matches between vertices that were not detected by the method outlined in the previous section. These inliers can be added to the set of matched vertices if the differences between the vertices are within the specified confidence interval. The adjustment is carried out in successive iterations as outliers are removed and inliers are added to the set of observed data points until the set of matching vertices remains unchanged. The parameters are then used to transform the datasets into a common domain and the information can be overlaid for comparison, as shown in Figure 8.

While this method presents the case for 2D data, the method can be extended to fully 3D data. In this case the Gauss-Helmert model can be used to define the transformation of the 3D data (Mikhail and Ackermann, 1976). A more rigorous refinement method, such as ICP can be applied to refine the alignment (Bae and Lichti, 2008).

Figure 8: The three data sets overlapping. Black represents the original drawings, blue was captured by the survey, green is the raw point cloud and red is the extract plans from the point cloud.

5 COMPARISON TO PLAN AND CONTROL SURVEY

In the presented case, the plans and point cloud were transformed into the common coordinate system defined by the survey data. For the matching of the plans to the survey and point cloud data, initially 24 vertices were matched with a standard error of 0.0595m. After the outliers and inliers detection method was applied, a total of 56 matches were isolated with a standard error of 0.0227m (a maximum of 0.0977m). The large values in the residuals were observed due to the deviations between the plans and the actual construction. Such large discrepancies can be seen in Figure 8. The point cloud to the survey dataset had much lower residuals, with a final standard error of 0.003m (a maximum of 0.005m). These values are close to the model accuracy and specification of the total station in reflector-less mode.

In general, the raw point cloud data conforms well to the survey data within the specified point uncertainties for the scanner (±6mm). For extracted modelled line segments from the point cloud, the average error was approximately 0.035m (with a maximum of 0.141m). These values were closer to the accuracy of the scanner (average of ±0.002m, less than 0.01m) where the wall comprised of a flat section with no features. The larger error values were caused by small features not being identified and removed from the surface segments, such as pictures, shallow recessed doors and windows, electrical outlets, etc. These off-plane features could be removed by increasing sampling density to detect such small features. However, if the observed differences between these features and the wall are less than the positional uncertainty of the scanner points, they may not be identifiable.

The assumption that the walls are orientated to the vertical direction can also cause larger errors. A 3D planar fit to an example wall resulted in a standard deviation of ±0.00197m, within scanner accuracy. When tested, the vertical alignment of the wall was out by an angle of 5’11”. This resulted in a 2D line fit having a standard error of ±0.00380m, larger than the true 3D planar fit. In general, the survey data and the point cloud are comparable to each other, but larger differences were seen when compared to the existing plans. This is mainly due to the changes being made after the drawings were submitted. These are easily detected from the point cloud data.

The last concern is for regions of missing data, as previously highlighted. One contributing factor was the narrow corridors creating sparse sampling regions and occlusion of sections of the wall. A higher sampling resolution and an increase number of setups may alleviate this problem. The other factor was that large sections of the walls in the test site are constructed of glass, which resulted in no sampled points being observed in these regions.

6 CONCLUSION

This paper presented a method for the automatic extraction of 2D drawings from point cloud data captured with a Leica ScanStation, and the comparison with a total station survey and as-built plan of the test site. The point coordinates from the total station were considered the ground truth and were utilized to gauge the accuracy of the laser scanner. Where the 2D line was successfully extracted, the laser scanner was illustrated to closely match the accuracies of the total station using the reflector-less mode measuring system. Problems with the automatic extraction procedure occur where there was insufficient point resolution, or when small features could not be clearly isolated. In addition, both 3D point clouds and the information from the total station differed slightly to the original design in some areas of the test-site. This was mainly due to the building structure being built quite different from the original plan.

ACKNOWLEDGEMENTS

This project was in part supported by the Australian Research Council (ARC) Linkage Infrastructure grant (LE0775672) and Prof. M. Bennamoun and his team at the University of Western Australia are appreciated for their hardware support. In addition, this work has been in part supported by Curtin University of Technology and the Cooperative Research Centre for Spatial Information, whose activities are funded by the Australian Commonwealth's Cooperative Research Centres

REFERENCES

Anderson J. M. and Mikhail E. M. (1998), Surveying: Theory and Practice, McGraw-Hill, 1167 pages

Bae K.-H. and Lichti D. D. (2008), "Automated registration of three dimensional unorganised point clouds", ISPRS Hournal of Photogrammetry and Remote Sensing 63(1) 36-54

Beinat A., Crosilla F., Visintini D. and Sepic F (2007), Automatic non parametric procedures for terrestrial laser point clouds processing. International Archives of the Photogrammetry, Remote Sensing and Spatial Information Sciences XXXVI(part 3/W40B), 1–6

Belton D. and Lichti D. D. (2006), Classification and segmentation of terrestrial laser scanner point clouds using local variance information. International Archives of the Photogrammetry, Remote Sensing and Spatial Information Sciences XXXVI(part 5), 44–49

Boehler W., Vincent M. B. and Marbs A. (2003), Investigating laser scanner accuracy, International Archives of Photogrammetry, Remote Sensing and Spatial Information Sciences, XXXIV(Part 5/C15), 696-701

Budroni A. and Böhm J. (2009), Toward automatic reconstruction of interiors from laser data. In Proceedings of 3D-ARCH Trento, Italy

Fischler M. A. and Bolles R. C. (1981), Random sample consensus: a paradigm for model fitting with applications to image analysis and automated cartography. Communications of the ACM 24 (6), 381–395

Frank T., Tertois A.-L. and Mallet J.-L. (2007), 3D-reconstruction of complex geological interfaces from irregularly distributed and noisy point data, Comput. Geosci., 33, 932–943

Froehlich C. and Metternleiter M. (2004), Terrestrial laser scanning – new perspectives in 3D surveying, International Archives of Photogrammetry, Remote Sensing and Spatial Information Sciences, XXXVI(Part 8/W2), 7 – 13

Golub G. H. and Loan C. F. V. (1989), Matrix Computations (2nd ed.). Baltimore, MD: Johns Hopkins Press.

Gordon S. J. (2005), Structural deformation measurement using Terrestrial Laser Scanners, Curtin University of Technology, Perth, Australia, PhD dissertation, 209 pages

Johnson R. A. and Wichern D. W. (2002), Applied Multivariate Statistical Analysis (5th ed.). New Jersey, USA: Prentice Hall.

Knuth D. E. (1999), The Art of Computer Programming, *Addison Wesley,* 896 pages

Leica-Geosystems (2011), http://www.leica-geosystems.com/ (Accessed August, 2011)

Lichti D. D., Franke J., Cannell W., and Wheeler K. D. (2005), “The Potential of Terrestrial Laser Scanners for Digital Ground Survey”, Journal of Spatial Science, Vol. 50(1), pp. 75-89

Lichti D. D. (2007), Error modeling, calibration and analysis of an AM-CW terrestrial laser scanner system, The ISPRS journal of Photogrammetry and Remote Sensing, 5, 307-324

Mikhail E. M. and Ackermann F. (1976), Observations and Least-Squares, IEP, 497 pages

Miliaresis G. and Kokkas N. (2007), Segmentation and object-based classification for the extraction of the building class from LIDAR DEMs, Comput. Geosci., 33, 1076–1087

Mólnar G., Pfeifer N., Ressl C., Dorninger P., and Nothegger C. (2009), Range calibration of terrestrial laser scanner with piecewise linear functions, Photogrammetrie, Fernerkundung, Geoinformation 2009 (1), 563-576

Okorn B., Xiong X., Akinci K. and Huber D. (2010), Toward automated modeling of floor plans. In Proceedings of 3D Data Processing, Visualization and Transmission (3DPVT) 2010

Pauly M., Gross M. and KobbeltL. P. (2002), Efficient simplification of point sampled surfaces. In VIS '02: Proceedings of the conference on Visualization '02, Boston, Massachusetts, 163–170. IEEE Computer Society.

Rabbani T. and van den Heuvel F. (2004), 3D Industrial Reconstruction by Ritting CSG Models to a Combination of Images and Point clouds. International Archives of Photogrammetry, Remote Sensing and Spatial Information Sciences XXXV.

Rabbani T., van den Heuvel F. A. and Vosselman G. (2006), Segmentation of point clouds using smoothness constraint. International Archives of the Photogrammetry, Remote Sensing and Spatial Information Sciences XXXVI(part 5), 248–253

Rüeger J. M. (1990), Electronic Distance Measurement, Springer-Verlag, Berlin, Germany

Schnabel R., Wahl R. and Klein R. (2007), Efficient RANSAC for point-cloud shape detection. Computer Graphics Forum 26 (2), 214–226

Schofield W. and M. Breach M. (2007), "Engineering Surveying", Elsevier, 622 pages

Shakarji C. M. (1998), Least-squares fitting algorithms of the NIST algorithm testing system. Journal of Research of the National Institute of Standards and Technology 103 (6), 633–641.

Sokkia (2011), http://www.sokkia.com/ (Accessed August, 2011)

Tarsha-Kurdi F., Landes T. and Grussenmeyer P. (2007), Hough-transform and extended RANSAC algorithms for automatic detection of 3d building roof planes from lidar data, in Proceedings of the ISPRS Workshop on Laser Scanning 2007, 407-412

Várady T., Benkö P. and Kós G. (1998), Reverse engineering regular objects: simple segmentation and surface fitting procedures. International Journal of Shape Modelling 4, 127–141

Vosselman G. and Dijkman S. (2001), 3D building model reconstruction from point clouds and ground plans. International Archives of the Photogrammetry, Remote Sensing and Spatial Information Sciences XXXIV (part 3/W4), 37–44

BRIEF BIOGRAPHY OF AUTHORS

David Belton is a research fellow with the CRC for Spatial Information at Curtin University, in the Department of Spatial Sciences. His research interests lie in laser scanning, 3D point cloud processing, error analysis, and optimisation techniques.

Brian Mooney received his BSurv degree from Curtin University in 2009. He is currently employed with Newmount Mining, Australia

Tony Snow is a Senior Lecturer and the undergraduate coordinator for surveying in the Department of Spatial Sciences, at Curtin University. His interests are in surveying principles and applications of emerging techniques and technology.

Kwang-Ho Bae works for Furgo Spatial Solutions as a laser scanning specialist. He was a lecturer in Photogrammetry and Laser Scanning in the Department of Spatial Sciences at Curtin between 2008 and 2011. His research interests are Laser Scanning data analysis such as registration, segmentation, calibration and positional error analysis, Photogrammetry and 3D range cameras.